The role of STEAP1 in the biological behavior of gastric cancer

Zhe Zhang
China Medical University
Wen-bin Hou
Sun Yat-Sen University
Chao Zhang
China Medical University
Dong-dong Zhang
China Medical University
Wen An
China Medical University
Si-wei Pan
China Medical University
Wan-di Wu
China Medical University
Qing-chuan Chen
China Medical University
Huimian Xu (xuhuimian123@163.com)
China Medical University Hospital https://orcid.org/0000-0002-1177-4445

Primary research

Keywords: STEAP1, Gastric cancer, Inflammatory reaction, Proliferation, Metastasis

Posted Date: June 15th, 2020

DOI: https://doi.org/10.21203/rs.3.rs-35114/v1

Abstract

Background: Six-transmembrane epithelial antigen 1 (STEAP1) is associated with the occurrence and development of cancer. This study aimed to clarify the role of STEAP1 in gastric cancer tumor growth and metastasis, as well as its molecular mechanism of action.

Methods: Statistical methods were used for clinical data analysis. Protein expression was detected using immunohistochemistry. The mRNA and protein expression in the cell cultures were detected using reverse transcription-polymerase chain reaction and western blot analysis. Overexpression and silencing models were constructed using plasmid and lentivirus transfection. To detect cell proliferation in vitro, Cell Counting Kit-8, flow cytometry, and colony formation assays were used; transwell and wound healing assays were used to detect cell migration and invasion; RNA sequencing was used for identifying differentially expressed genes; ELISA assay was used to detect the secretory proteins in cells. For in vivo experiments, nude BALB/c mice were used for detecting subcutaneous tumorigenesis and intraperitoneal implantation.

Results: STEAP1 was overexpressed in gastric cancer tissues and cell lines. Single factor and Cox analyses showed that STEAP1 gene expression level correlated with poor prognosis. Upregulation of STEAP1 increased cell proliferation, migration, and invasion, which decreased after STEAP1 was knocked down. These changes were achieved via the activation of the AKT/FoxO1 pathway and epithelial-mesenchymal transformation (EMT). The RNA sequencing results indicated that STEAP1 was closely related to inflammatory reactions. STEAP1 can regulate the inflammation-related molecules, IL-1β and IL-6, via the NF-kB and ERK/c-Jun signaling pathways. The in vivo animal experiments showed that STEAP1 knock down, resulted in a decrease in the subcutaneous tumor and peritoneal tumor formation.

Conclusion: STEAP1 was overexpressed in gastric cancer and closely associated with OS. STEAP1 can regulate the cell cycle via the Akt/FoxO1 pathway to influence cell proliferation. STEAP1 may affect cell migration and invasion via EMT action. In addition, STEAP1 may mediate the inflammatory response by regulating IL1β and IL6 via the NF-kB and the ERK/c-Jun signaling pathways.

Background

Gastric cancer is a common kind of malignant tumor that seriously affects people's health.[1] According to the data from the World health Organization (WHO), in contrast to the United States, Australia and New Zealand, China, Japan, and Chile have higher incidence areas of gastric cancer.[2] In China, gastric cancer is the second cause of cancer-related deaths, with 679000 new cases and 498000 deaths.[3] Gastric cancer is predisposed to occur in individuals aged between 50 and 70 years. However, in recent years, it has shown a "younger" trend.[4-9] Therefore, it is essential to find new tumor markers to predict the risk of gastric cancer progression.

Tumor development involves many factors, which are controlled by many genes, including prostate transmembrane epithelial antigen. Six-transmembrane epithelial antigen (*STEAP*) was found as a

prostate-specific cell surface antigen using suppression subtractive hybridization technique for the first time[10,11]. STEAP is highly expressed in spontaneous transgenic mouse prostate cancer models and human prostate cancer. In addition, it is also expressed in the pancreas, ovary, gastrointestinal tract, cervix, testis, bladder, Ewing sarcoma, and melanoma cells[10,12]. There are four members in the STEAP protein family, STEAP1-4. The main focus of our study is STEAP1.

Gene *STEAP1* is located in the 7q21.13 region of the human chromosome; it is 10.4 kb long and contains four introns and five exons. The transcription of the gene *STEAP1* can produce two different kinds of mRNAs: a 1.4 kb and a 4 kb mRNAs. However, only the 1.4 kb mRNA can be processed into a mature protein, which contains 339 amino acids with molecular weight of 36 KD.[10,12], while the 4 kb mRNA contains a 2399 BP large intron, which is not translated into a mature protein. Data has shown that gene *STEAP1* is closely related to communication between the adjacent cells, and it seemed to be beneficial for the occurrence and development of tumors.[13] Its structural prediction and the location at the cell-cell contacts indicated that gene *STEAP1* product may be a transporter or channel.[10,14] Some previous research on different kinds of cancer have found that *STEAP1* was observed in tumor tissue but not in normal tissue. The expression of *STEAP1* was closely related to the malignant phenotype of cancer cells. [15-20] However, in Lee's study, they found no correlation between expression of *STEAP1* and the clinicopathological factors.[21] These conflicting results indicated that the roles of *STEAP1* were varied depending on different cancer types. In our study, we will discuss the influence of *STEAP1* on the proliferation, invasion, and inflammatory reactions in gastric cancer.

Materials And Methods

2.1 Clinical samples

212 samples of gastric cancer tissue and 60 samples of adjacent normal gastric tissue from patients were obtained from the First Affiliated Hospital of China Medical University from 2003 to 2010. None of the patients received preoperative chemotherapy or radiotherapy, and all of them were proven to have gastric cancer by pathology. The cancer tissue was fixed with formalin and preserved in paraffin. All pathological data were complete, and the postoperative follow-up was sufficient. All patients were approved by the ethics committee of China Medical University to participate in the study and provided written informed consent.

2.2 Immunohistochemistry of human gastric cancer

To fix gastric cancer tissue samples, 10% formalin was used, then the tissue was paraffin-embedded and cut into 4-μm slices. The xylene and alcohol were used for dewaxing and rehydrating. Endogenous peroxidase activity was blocked by using hydrogen peroxide (30%), the citrate buffer (pH 6.0) was used to boil the the sections fro 3 minutes in a pressure cooker. Next, normal goat serum was used for incubating the sections to reduce the nonspecific binding. Finally, the tissue sections were incubated (4°C, 12 h) with anti-STEAP1 antibody (1:200 dilution, B-4, SC-271872, Santa Cruz, USA). Finally, the sections were stained with diaminobezidin (DAB) for 60 sec, stained with hematoxylin for 2 min and sealed with neutral

resin. Two pathologists examined all tumor slides randomly. We evaluated STEAP1 staining intensity as follows: scored 0 (negative), 1 (weakly negative), 2 (weak positive), and 3 (strong positive). The percentage scores of positive cells per single field vision were as follows: scored 1 (0-25%), 2 (26-50%), 3 (51-75%), and 4 (76-100%). We multiplied the two scores above and obtained a final score ranging from 0 to 12. Tumor samples with a score <6 were considered as negative expression; on the contrary, the score ≥6 was considered as positive expression.

2.3 Animals

Twenty-four BALB/c nude female mice were purchased from Beijing Vital River Laboratory Animal Technology Co., Ltd. The mice were raised in the animal experimental center of of China Medical University. The twenty-four nude mice were randomly divided into four groups. Two groups were used for hypodermic injection, and the other two groups were intraperitoneally injected with 3×10^6 cells per nude mouse. All animal experimental steps were approved by the Animal Research Committee of China Medical University.

2.4 Cell culture

GES-1, a normal gastric mucosa cell line was obtained from Nanjing Cobioer Biotechnology Co., Ltd. The gastric cancer cell lines MGC-803 and SGC-7901 were obtained from the Chinese Academy of Sciences. AGS was purchased from the American Type Culture Collection (ATCC, Manassas, VA, USA). MGC-803, SGC-7901 and GES-1 cells were cultured in DMEM containing 10% FBS. AGS line was cultured in DMEM-F12 medium containing 10% FBS. All cells were cultured at 37°C in a 5% CO2 incubator.

2.5 Cell transfection

ShRNA lentivirus was purchased from Shanghai Genechem Co., Ltd. The NC group insertion sequence was TTCTCCGAACGTGTCACGT. There were three shRNA sequences used (shRNA1: CCAACTTCATAATGGAACCAA; shRNA2: CAGCACACACAGGAACTCTTT; and shRNA3: AAGCTAGGAATTGTTTCCCTT). The *STEAP1* containing cDNA plasmid and Flag empty plasmid were purchased from Beijing SinoBiological Co., Ltd. Lipofectamine 3000 reagent (Thermo Fisher Scientific, Inc.) was used for plasmid transfection. The cells were harvested 48 h after transfection. Western blot analysis and RT-PCR were used to check the transfection efficiency.

2.6 RT-PCR

TRIzol reagent was used to extracted total RNA. The reverse transcription kit PrimeScript RT was purchased from Takara. The primer designs were provided by Huada Gene Co., and the sequences were as follows: GAPDH, 5’-GTCTCCTCTGACTTCAACAGCG-3’ (forward), 5’-ACCACCCTGTTGCTGTAGCCAA-3’ (reverse); β-actin, 5’-CACCATTGGCAATGAGCGGTTC-3’ (forward), 5’-AGGTCTTTGCGGATGTCCACGT-3’ (reverse); CCND1, 5’-TCTACACCGACAACTCCATCC-3’ (forward), 5’-TCTGGCATTTTGGAGAGGAAGTG-3’ (reverse); P27, 5’-ATAAGGAAGCGACCTGCAACCG-3’ (forward), 5’-TTCTTGGGCGTCTGCTCCACAG-3’

(reverse); CDK4, 5′-CTCGTGCTGATGCTACTGAGGA-3′ (forward), 5′-GGTCGGCGCAGTTGGGCTCC-3′ (reverse); E-cadherin, 5′-GCCTCCTGAAAAGAGAGTGGAAG-3′ (forward), 5′-TGGCAGTGTCTCTCCAAATCCG-3′ (reverse); N-cadherin, 5′-CCTCCAGAGTTTACTGCCATGAC-3′ (forward), 5′-GTAGGATCTCCGCCACTGATTC-3′ (reverse); MMP-2, 5′-AGCGAGTGGATGCCGCCTTTAA-3′ (forward), 5′-CATTCCAGGCATCTGCGATGAG-3′ (reverse); MMP9, 5′-GCCACTACTGTGCCTTTGAGTC-3′ (forward), 5′-CCCTCAGAGAATCGCCAGTACT-3′ (reverse); IL1β, 5′-CCACAGACCTTCCAGGAGAATG-3′ (forward), 5′-GTGCAGTTCAGTGATCGTACAGG-3′ (reverse); and IL6, 5′-AGACAGCCACTCACCTCTTCAG-3′ (forward), 5′-TTCTGCCAGTGCCTCTTTGCTG-3′(reverse).

2.7 Western blot analysis

All proteins were obtained by lysing the cells. Proteins were separated using sodium dodecyl sulfate-polyacrylamide gel electrophoresis (SDS-PAGE, 8%). After transferring to a polyvinylidene fluoride (PVDF) membrane (Millipore, Billerica, MA, USA), the membranes were incubated overnight at 4°C with antibodies against STEAP1 (SC-271872, 1:400) from Santa Cruz, USA. The other antibodies used are as follows. GAPDH (60004-1-Ig, 1:10000), β-actin (60008-1-Ig, 1:10000), IL1β (16806-1-AP, 1:1000), IL6 (66146-1-Ig, 1:1000), and NF-kB (14220-1-AP, 1:1000) were purchased from Proteintech Group, Wuhan, China. P27 (3686, 1:1000), CDK4 (2546, 1:1000), AKT (4691, 1:1000), P-AKT (4060, Ser473, 1:2000), FoxO1 (2880, 1:1000), P-foxO1 (9464, 1:2000), E-cadherin (14472, 1:1000), N-cadherin (13116, 1:1000), Vimentin (5741, 1:1000), MMP-2 (4022, 1:1000), MMP9 (13667, 1:1000), c-Jun (9165,1:1000), P-c-Jun (3270, 1:2000), Erk (4695, 1:1000), and P-Erk (4370, 1:2000) were purchased from Cell Signaling Technology, USA. P-NF-kB (109458, 1:3000) was purchased from Abcam, UK. Then the goat anti-rabbit and anti-mouse IgG secondary antibodies were used to incubate the membrane at room temperature for 60 min. Finally, the ECL was used to visualize and detect the proteins by using BioImaging Systems (UVP Inc., Upland, CA, USA).

2.8 Cell Counting Kit-8 (CCK-8) assay

SGC-7901 and MGC-803 cells were transfected with an empty vector, *STEAP1* plasmid, negative control virus, or sh-STEAP1 virus. Cells were seeded at 3000 per well into a 96-well plate, and CCK-8 solution (Beyotime, Shanghai, China) was added into every well at 24h, 48h, 72h and 96 h. A microplate reader was used to measure the absorbance values and estimate the cell proliferation rates.

2.9 Colony formation assay

For the colony formation assay, SGC-7901 and MGC-803 cells were transfected with plasmid or shRNA for 36 h and plated into 6-well cell plates (1000 cells/well). The cells were cultured in a 37°C incubator for 2-3 weeks, fixed with alcohol for 30 min, and stained with Trypan Blue for 20 min at room temperature. The colonies with more than 50 cells were counted. Finally, an HD camera was used to obtain the images.

2.10 Flow cytometry

We used a flow cytometry assay to detect the cell cycle stage. SGC-7901 and MGC-803 cells were transfected with plasmid or shRNA and plated into 6-well plates (1×10^5 cells/well). After 24 h, the cells were harvested using 0.25% trypsin in 1.5 ml Eppendorf tubes. Then, the cells were stained with propidium iodide (PI, 500 μ/tube, KeyGEN, Nanjing, China) at 37°C in the dark for 30 min. Finally, the cells were analyzed using a FACSCalibur flow cytometer (Becton Dickinson, USA).

2.11 Transwell assay

Cell migration experiments were performed using a 24-well transwell chamber with a pore size of 8 μm (Costar). A total of 5×10^4 cells in serum-free DMEM were placed in the upper chamber, and DMEM with 10% FBS was added to the lower chamber. After more than 10 hours, the migration experiment was terminated, and the cells were observed in the medium below. Then, the cells on the membrane in the bottom chamber were fixed with 75% alcohol for 30 min and stained with Trypan Blue at room temperature for 20 min. Images were obtained using an inverted microscope. In addition, the transwell chamber was also used for cell invasion experiments. For these experiments, in addition to the above steps, Matrigel (1:9 dilution, BD Bioscience) was added to the upper chamber to observe the change in cell invasion ability.

2.12 Wound healing assay

A wound healing assay was used to observe the migration of cells. In this study, 1×10^5 cells were seeded into 6-well plates for every group. After the cells had covered the entire plate, a pipette tip was used to make a scratch in the cell monolayer, and phosphate buffer saline (PBS) was used to wash the floating cells three times. Subsequently, we used serum-free DMEM instead of the former medium. Finally, an inverted microscope (Olympus, Japan) was used to take images at 0 h and 96 h. The difference in scratch distance between the two phases can reflect the difference in the cell migration ability.

2.13 ELISA assay

The ELISA assay can be used to detect the amount of secretory proteins in cells. Cells in each group were seeded into 6-well culture plates at a density of 1×10^6 cells/well. Two milliliters of DMEM with 10% FBS were used to culture the cells. After 48 h, the cell culture medium was collected, and the secretory proteins were detected using an ELISA kit (VAL101; VAL102, R&D Systems, MN, USA). The procedures were performed according to the manufacturer's instructions.

2.14 Statistical analysis

GraphPad Prism 7.0 was used for image editing. The data were expressed as the means±SEMs. SPSS 21.0 statistical software was used for data analysis. The chi-square test was used to examine possible correlations between STEAP1 expression and clinicopathological factors. Survival rates were calculated using Kaplan-Meier analysis. The log-rank test was used for single-factor analysis. Cox risk proportion model was used for multi-factor analysis, and a value of $P<0.05$ was considered statistically significant.

Results

3.1 STEAP1 was highly expressed in gastric cancer tissue and closely connected with OS.

The GEPIA database showed that the STEAP1 gene was more highly expressed in gastric cancer than in the normal tissue (Fig. 1A). We detected 212 cases of gastric cancer tissues and 60 cases of paracancerous tissues using IHC and scored them. The results showed that STEAP1 was highly expressed in cancer tissues and was mainly localized to the membrane and cytoplasm in cells (Fig. 1B). The positive expression rate of STEAP1 was 54.7% (116/212). However, it was expressed at low levels or was negative in paracancerous tissues (Fig. 1C). The 5-year OS in the high expression group was 25.9%, which was significantly lower than 60.7% in patients with low expression group (P<0.0001, Fig. 1D). Fig. 1E shows the detailed score in 212 cases of tumor tissues and in 60 cases of paracancerous tissues. The scores between the two groups were significantly different (P<0.0001). In addition, 60 matched tissues were scored, and the details are shown in Fig. 1F (P<0.0001). The subsequent study of the data of 212 clinical cases showed that the factors that affected the prognosis in patients included tumor location (P=0.029), tumor size (P=0.012), Borrmann type (P=0.019), STEAP1 expression (P<0.001), N stage (P<0.001), T stage (P<0.001), and distant metastasis (P=0.005) (Table 1). Cox multifactor analysis showed that the independent factors influencing the prognosis of patients included STEAP1 expression (P<0.001), T stage (P=0.005), and N stage (P<0.001) (Table 2). In the study of the relationship between the expression of STEAP1 and clinicopathological factors, high expression of STEAP1 was closely related to Borrmann type (P=0.009) and N stage (P<0.001) (Table 3).

3.2 Screening of the experimental cell lines and knockdown virus transfection

We detected the STEAP1 mRNA level in GES-1, AGS, SGC-7901, and MGC-803 cells using RT-PCR (Fig. 1G). The results showed that STEAP1 was more highly expressed in SGC-7901 and MGC-803 cells. The western blot analysis yielded the same conclusion (Fig. 1H). Therefore, we selected SGC-7901 and MGC-803 cells as experimental cell lines. We overexpressed and knocked down the STEAP1 gene by transfecting the *STEAP1* plasmid and *STEAP1* shRNA. We transfected negative control (NC) virus and three kinds of *STEAP1*-shRNAs into SGC-7901 cells and detected the knockdown efficiency on mRNA and protein levels using RT-PCR and western blot analysis. The results showed that shRNA2 had the highest knockdown efficiency (Fig. 1I). Subsequently, we transfected NC virus and STEAP1-shRNA2 into SGC-7901 and MGC-803 cells. The results showed successful transfection and knockdown using RT-PCR and western blot analysis (Fig. 1J-K).

3.3 STEAP1 gene regulates the cell cycle via the Akt/FoxO1 pathway to influence cell proliferation.

The CCK-8 assay results showed that the absorbance in the sh-STEAP1 group was lower than that in the NC group at 48 h, 72 h, and 96 h in both the SGC-7901 and MGC-803 cell lines (Fig. 2A). In another group of comparisons, we found that the absorbance of the STEAP1 plasmid vector group was higher than that of the NC group at 24 h, 48 h, 72 h, and 96 h in both the SGC-7901 and MGC-803 cell lines (Fig. 2B). The CCK-8 results indicated that the STEAP1 gene can influence cell proliferation. When STEAP1 was

overexpressed, cell proliferation increased. When STEAP1 was knocked down, cell proliferation decreased. In the colony formation assay, we found that when STEAP1 was knocked down, the colony number was lower than that in the NC group (Fig. 2C), while when STEAP1 was overexpressed, the colony number was higher than that in the empty vector group (Fig. 2D). The experimental results were consistent in the SGC-7901 and MGC-803 cell lines. The colony formation assay results also indicated that the STEAP1 gene can influence cell proliferation. When STEAP1 was knocked down, cell proliferation decreased, and when STEAP1 was overexpressed, cell proliferation increased. Next, we used flow cytometry to detect the cell cycle. The results showed that when STEAP1 was knocked down, the percentage of the cells in S phase was decreased, and the percentages of cells in G0/G1 and G2/M phase was increased in both SGC-7901 and MGC-803 cells (Fig. 2E). When STEAP1 was overexpressed, the percentage of S phase cells was increased, and the percentages of G0/G1 and G2/M phase cells was decreased in both SGC-7901 and MGC-803 cells (Fig. 2F). The flow cytometry assay indicated that the *STEAP1* gene can influence cell proliferation by influencing the cell cycle. Finally, we detected cell cycle related proteins and pathway proteins to identify the underlying mechanism. The Western blot analysis showed that when STEAP1 was down regulated, CDK4 and Cyclin D1 were relatively down regulated, and P27 was upregulated. Total AKT (AKT) and total FoxO1 (FoxO1) showed no significant change, while phosphorylated AKT (P-AKT) was down regulated, and phosphorylated FoxO1 (P-FoxO1) was upregulated (Fig. 2G). When STEAP1 was upregulated, CDK4 and Cyclin D1 were relatively upregulated, and P27 was down regulated. AKT and FoxO1 also showed no significant change, while P-AKT was upregulated and P-FoxO1 was down regulated (Fig. 2H).

3.4 STEAP1 regulates cell migration and invasion via EMT.

The transwell assay results showed that the number of migrating cells in the sh-STEAP1 group was lower than that in the NC group in both SGC-7901 and MGC-803 cells (Fig. 3A). The number of migrating cells in the STEAP1 plasmid group was higher than that in the empty vector group (Fig. 3B). The results of the wound healing assay also provided consistent conclusions. In SGC-7901 cells, the migration distance between 0 h and 96 h in the NC group was more obvious than that in the sh-STEAP1 group. The migration distance of the empty vector group was shorter than that of the STEAP1 plasmid group (Fig. 3C). This result was also identified in MGC-803 cells. The migration distance of the NC group was longer than that of the sh-STEAP1 group, and the migration distance of the empty vector group was shorter than that of the STEAP1 plasmid group (Fig. 3D). The results of the above two experiments indicated that when STEAP1 was knocked down, the cell migration ability was decreased, whereas it increased after the overexpression of STEAP1. We also used a transwell assay and placed Matrigel into the upper chamber for detecting the effect of the STEAP1 gene on cell invasion. The results showed that the number of invading cells in the sh-STEAP1 group was lower than that in the NC group in both SGC-7901 and MGC-803 cells (Fig. 3E). The number of invading cells in the STEAP1 plasmid group was higher than that in the empty vector group (Fig. 3F). These results indicated that the STEAP1 gene had an effect on cell invasion. When STEAP1 was knocked down, the cell invasion ability was decreased and increased after overexpressing STEAP1. Finally, we detected cell migration- and invasion-related proteins using western blot analysis. The results showed that N-cadherin, MMP-2, and MMP-9 were downregulated and E-

cadherin was upregulated after we downregulated the gene STEAP1 (Fig. 3G). In contrast, when STEAP1 was overexpressed, Vimentin, N-cadherin, MMP-2, and MMP-9 were relatively upregulated, and E-cadherin was downregulated (Fig. 3H).

3.5 STEAP1 mediates the inflammatory response by regulating IL1β and IL6 via the NF-kB and ERK/c-Jun signaling pathways.

To investigate the effect of STEAP1 on other genes, we analyzed the differentially expressed genes between the SGC-7901 NC group and the sh-STEAP1 group using RNA sequencing. The complete results are shown in the volcano map (Fig. 4A). We used a heat map to analyze inflammation-related genes and found that there was a significant difference between the two groups in IL-1β and IL-6 (Fig. 4B-C). As it is known from the literature, there are two main pathways that can regulate IL-1β and IL6.The first one is NF-kB pathway, and the other is Erk/c-Jun pathway. We hypothesized that STEAP1 can regulate IL-1β and IL6 through these two pathways to mediate inflammation. Therefore, we analyzed IL-1β, IL-6, and their upstream regulatory pathway proteins using Western blot. The results showed that when we downregulated STEAP1, the protein expression of IL-1β and IL6 was decreased. As upstream related pathway proteins, total Erk had no change, while total c-Jun, phosphorylated Erk (P-Erk), and phosphorylated c-Jun (P-c-Jun) levels were decreased. The level of the other pathway protein, the expression of total NF-kB (NF-kB) had no change, while phosphorylated NF-kB (P-NF-kB) was decreased (Fig. 4D). In contrast, when we upregulated STEAP1, the protein expression of IL-1β and IL6 levels were increased. As upstream regulatory pathway proteins, total Erk level still was not changed, while total c-Jun, P-Erk, and P-c-Jun levels were increased. Similarly, the level of the other pathway protein, the expression of total NF-kB was not changed, while P-NF-kB levels were increased (Fig. 4E). Considering that IL-1β and IL6 are secretory proteins, it is necessary to detect the changes in these proteins secretion in cell culture medium. We used ELISA kits to detect the amount of IL-1β and IL-6 secreted by the cells. The results showed that when STEAP1 was knocked down, the secretion of IL-1β was decreased and it was increased after overexpressing STEAP1 in both SGC-7901 and MGC-803 cells (Fig. 4F). The IL-6 levels analysis showed similar results. When STEAP1 was knocked down, the secretion of IL-6 was decreased and it was increased in response to STEAP1overexpression (Fig. 4G). These results indicated that STEAP1 may mediate the inflammatory response by regulating IL1β and IL6 via the NF-kB and Erk/c-Jun signaling pathways (Fig. 4H).

3.6 In vivo animal experiments

Twelve BALB/c nude mice were used to study tumor formation and were randomly divided into two groups. We subcutaneously injected 3×10^6 of SGC-7901 NC cells per mouse in the first group, which was called the NC group. The mice in the other group were subcutaneously injected with 3×10^6 of SGC-7901 and sh-STEAP1 cells per mouse, which was called sh-STEAP1 group. The tumor sizes were measured every 2 days from 4 to 14 days after the injection and the results are shown in Fig. 5B. Twelve tumor specimens were removed from the mice on the 14th day. The results showed that the tumor size in the NC group was larger than that in the sh-STEAP1 group (Fig. 5A). Next, we observed the expression of

STEAP1, Ki-67, cleaved caspase3, IL-1β, and IL-6 in IHC experiments. We found that the expression of STEAP1 in NC group was higher than in the sh-STEAP1 group (Fig. 5C). This result showed that the silencing efficiency of STEAP1 in tumor was still very high. The expression of Ki-67 in NC group was higher than that in the sh-STEAP1 group (Fig. 5D), while the expression of the cleaved caspase3 in NC group was lower than that in the sh-STEAP1 group (Fig. 5E).These results above also confirmed that STEAP1 can affect the proliferation of gastric cancer cells in vivo. In addition, we also found that the expression levels of IL-1β and IL-6 in NC group were higher than sh-STEAP1 group (Fig. 5F-G). In the intraperitoneal tumorigenesis experiment, twelve mice were divided into the NC and sh-STEAP1 groups, and 3×10^6 cells per mouse were injected by intraperitoneal injection. Three weeks later, the mice were sacrificed to observe peritoneal tumorigenesis. The results showed that the number of tumors in the NC group was significantly higher than that in sh-STEAP1 group (Fig. 5H-I). We observed that the tumors were mainly located on the mesentery and the intestinal wall (Fig. 5J). There was significant difference in the number of tumors between the two groups (Fig. 5K).

Discussion

As a global health problem, cancer affects the quality of patients' lives worldwide and causes thousands of deaths every year.[1] It is necessary to find new indicators to predict the occurrence and development of cancer. STEAP1 was found through suppression subtractive hybridization at the first time. A number of previous research studies found that it was over expressed in many kinds of cancers, such as prostate, colon, bladder, ovarian, pancreatic, testicular, breast, cervical cancers, and Ewing sarcoma[10,12]. However, there are few studies on this gene in the field of gastric cancer, and no one has explored its effect on biological function and mechanisms of action. In this research, a detailed exploration of tumor proliferation, migration, and invasion with regard to the role of STEAP1 in the biological behavior of gastric cancer cells was carried out. Moreover, we also found that STEAP1 was closely related to the expression of some inflammatory factors.

In our study, STEAP1 was overexpressed in gastric cancer and closely associated with patient prognosis. The 5-year OS in patients with a low expression of STEAP1 was 60.7%, while that in patients with high STEAP1expression was only 25.9% (Fig. 1D). STEAP1 plays an oncogenic role in gastric cancer, and this result was consistent with the conclusion that STEAP1 is an oncogene in other kinds of cancer. Tumor cell growth, metastasis, proliferation, migration and invasion are basic biological functions.[22] We downregulated or upregulated STEAP1 using lentivirus knockdown or STEAP1 plasmids, respectively, to detect the changes in the above mentioned functions. The results obtained with the CCK-8 and colony formation assays indicated that when we overexpressed STEAP1, the percentage of cells in the S phase was increased, and that in the G0/G1 and G2/M phases was decreased, and the cell proliferation ability was also improved. In contrast, when STEAP1 was knocked down, the percentage of cells in the S phase was decreased, while that in the G0/G1 and G2/M phases was increased, and cell proliferation was reduced (Fig. 2A-F). Cyclin D1 is known as an oncogene and it is overexpressed in many kinds of cancers. [23] By binding with CDK4 (a partner kinases of cyclin D1), cyclin D1 can release transcription factors and

advance cell cycle progression from the G1 phase to the S phase. The P27 protein limits cell cycle progression, mainly by inhibiting complex formation, such as Cyclin D1-CDK4 and CyclinE-CDK2, to block the cell cycle in the G1 phase. Previous studies have found that the AKT pathway is one of the main signaling pathways influencing cancer cell proliferation.[24-29] Therefore, it was reasonable to consider that STEAP1 can affect cell proliferation via the AKT pathway. Our results also showed that when STEAP1 was downregulated, P-AKT, CDK4, and Cyclin D1 were relatively downregulated, and P27 and P-FoxO1 were upregulated (Fig. 2G). When STEAP1 was upregulated, P-AKT, CDK4, and Cyclin D1 were relatively upregulated, and P-FoxO1 and P27 were downregulated. P-AKT was upregulated and P-FoxO1 was downregulated (Fig. 2H). These results indicated that STEAP1 can regulate the cell cycle via the Akt/FoxO1 pathway to influence cell proliferation.

The results of the transwell and wound healing assays showed that when we overexpressed STEAP1, cell migration and invasion increased. In contrast, when STEAP1 was knocked down, these two abilities were decreased (Fig. 3A-F). Therefore, we can conclude that STEAP1 had an effect on the migration, invasion, and metastasis in gastric cancer cells. Epithelial mesenchymal transition (EMT) refers to the cells that lost the characteristics of epithelial cells and acquired the characteristics of mesothelial cells. Subsequently, the abilities of cell invasion and metastasis were enhanced. The EMT-related proteins include N-cadherin, vimentin, and E-cadherin. A previous study showed that when cells tended to migrate and metastasize, the protein expression levels of vimentin and N-cadherin increased and those of E-cadherin decreased.[30,31] In addition, many studies have identified that metalloproteinase family plays a key role in tumor invasion and metastasis because of its ability of degrading extracellular matrix and destroying the histological barrier which can prevent tumor cell invasion. Among them, matrix metalloproteinase-2 (MMP2) and matrix metalloproteinase-9 (MMP9) are the most studied currently.[32-34] Therefore, EMT-related proteins, MMP2 and MMP9 were detected using western blot. The results showed that when STEAP1 was overexpressed, N-cadherin, Vimentin, MMP-2, and MMP-9 were relatively upregulated, and E-cadherin was downregulated. When STEAP1 was downregulated, N-cadherin, MMP-9, and MMP-2 were downregulated, and E-cadherin was upregulated (Fig. 3G-H). These results indicated that the STEAP1 gene may regulate cell migration and invasion via EMT.

Many studies have shown that inflammation was closely related to the occurrence and development of tumors. Inflammation can help to obtain a variety of marker functions by providing biological active molecules to tumor microenvironment. In the early stage of tumor evolution, inflammation can promote the early tumor to develop into a fully mature cancer and accelerate its transformation to a highly malignant tumor state. In the study of pyogenic dermatosis, STEAP1 was found to be overexpressed in patients' skin and co-localized with IL-36γ around neutrophils.[35] In our study, we analyzed differential gene expression between 7901 NC group and sh-STEAP1 group using RNA-seq. We found that STEAP1 was closely related to the expression of some inflammatory factors (Fig. 4C). Among these factors, we finally chose IL-1β and IL-6 as the candidate genes fur further investigation based on the following points. Firstly, we found that the differences in IL-1β and IL-6 levels between NC and sh-STEAP1 group were more than 4x and this difference was significant from the chart (Fig. 4C. $\log_2$<-2, P<0.05). Secondly,

IL-1β and IL-6 are the most studied inflammatory factors at present. Because of the substantial research done on these proteins, there is a range of reagents such as antibodies and ELISA kits available. Many studies have suggested that there are two upstream pathways can regulate IL-1β and IL-6. One is NF-kB pathway, and the other one is Erk/c-Jun pathway. We asked whether STEAP1 can regulate IL-1β and IL-6 via these two pathways. The result of Western blot analysis confirmed our conjecture (Fig. 4D-E). Indeed, STEAP1 may mediate the inflammatory response by regulating IL1β and IL6 via the NF-kB and Erk/c-Jun pathways (Fig. 4H).

As we know from the previous research, Ki67 can reflect the proliferation of tumor cells, with higher expression of Ki67 being correlated with stronger proliferation in tumor cells. Cleaved caspase3 is a key executor of apoptosis, the lower expression of cleaved caspase3, the less likely that the cells will undergo apoptosis. In our study, the analysis of the apoptosis marker cleaved caspase3 and proliferation-related nuclear antigen Ki-67 with IHC assay also indicated that STEAP1 plays a very important role in cell proliferation in vitro. As it is well known, peritoneal metastasis is the most important mechanisms of gastric cancer metastasis. Until the early 1990s, we always admitted that peritoneal metastasis of gastric cancer was a kind of terminal disease and the effect of systemic chemotherapy had limited effects on it. [36] In our study, we established a peritoneal metastasis model using intraperitoneal injection of tumor cells into nude mice. The results of these in vivo experiment showed that the number of tumors on the mesentery in the NC group was higher than that in the sh-STEAP1 group. We can also conclude that STEAP1 may affect the ability of intraperitoneal tumor to spread and get implanted into distant organs.

Limitations

In this paper, we discussed the effect of STEAP1 on the function of gastric cancer cells from many different aspects, but the mechanism of intermolecular interaction remained unclear. Next, we will continue to study the interaction sites between STEAP1 and other molecules.

Conclusions

In conclusion, STEAP1 was overexpressed in gastric cancer and closely connected with OS. STEAP1 can regulate the cell cycle via the Akt/FoxO1 pathway to influence cell proliferation. STEAP1 may affect cell migration and invasion via EMT induction. In addition, STEAP1 may mediate the inflammatory response by regulating IL1β and IL6 via the NF-kB and the ERK/c-Jun signaling pathways.

Abbreviations

STEAP1 Six-transmembrane epithelial antigen 1

IHC Immunohistochemistry

RT-PCR Reverse Transcription-Polymerase Chain Reaction

CCK-8 Cell Counting Kit-8

ELISA Enzyme linked immunosorbent assay

EMT Epithelial mesenchymal transformation

DAB Diaminobezidin

PBS Phosphate buffered saline

Declarations

Ethics approval and consent to participate

All patients were approved by the ethics committee of China Medical University to participate in the study and provided written informed consent. All animal experimental steps were approved by the Animal Research Committee of China Medical University.

Consent for publication

Not applicable

Availability of data and materials

Not applicable

Competing interests

There are no competing interests to declare

Funding

This work was supported by National Natural Science Foundation of China (No.81602522).

Author contributions

Project design: Hui-mian Xu, Wen-bin Hou, Zhe Zhang

Clinical data collection：Zhe Zhang

Cell function experiment： Dong-dong Zhang, Wen An

Animal experiment：Zhe Zhang, Chao Zhang

Data statistics and analysis：Si-wei Pan, Qing-chuan Chen

Manuscript writing and submission：Zhe Zhang, Wan-di Wu

Acknowledgements

We would like to thank Editage (www.editage.com) for English language editing.

References

1. Pisani P, Parkin DM, Bray F, Ferlay J. Estimates of the worldwide mortality from 25 cancers in 1990. Int J Cancer. 1999; 83(1):18-29.
2. Berardi R, Scartozzi M, Romagnoli E, Antognoli S, Cascinu S. Gastric cancer treatment: a systematic review. Oncol Rep. 2004;11(4):911-6.
3. Zong L, Abe M, Seto Y, Ji J. The challenge of screening for early gastric cancer in China. Lancet. 2016;388(10060):2606.
4. Jia B, Liu H, Kong Q, Li B. RKIP expression associated with gastric cancer cell invasion and metastasis. Tumour Biol. 2012;33(4):919-25.
5. Mayer B, Funke I, Johnson JP. High expression of a Lewis(x)-related epitope in gastric carcinomas indicates metastatic potential and poor prognosis. Gastroenterology. 1996;111(6):1433-46.
6. Jia Y, Dong B, Tang L, Liu Y, Du H, Yuan P, et al. Apoptosis index correlates with chemotherapy efficacy and predicts the survival of patients with gastric cancer. Tumour Biol. 2012;33(4):1151-8.
7. Oishi Y, Watanabe Y, Yoshida Y, Sato Y, Hiraishi T, Oikawa R, et al. Hypermethylation of Sox17 gene is useful as a molecular diagnostic application in early gastric cancer. Tumour Biol. 2012; 33(2):383-93.
8. Janjigian YY, Werner D, Pauligk C, Steinmetz K, Kelsen DP, Jager E, et al. Prognosis of metastatic gastric and gastroesophageal junction cancer by HER2 status: a European and USA International collaborative analysis. Ann Oncol. 2012;23(10):2656-62.
9. Yu J, Cheng YY, Tao Q, Cheung KF, Lam CN, Geng H, et al. Methylation of protocadherin 10, a novel tumor suppressor, is associated with poor prognosis in patients with gastric cancer. Gastroenterology. 2009;136(2):640-51 e1.
10. Hubert RS, Vivanco I, Chen E, Rastegar S, Leong K, Mitchell SC, et al. STEAP: a prostate-specific cell-surface antigen highly expressed in human prostate tumors. Proc Natl Acad Sci U S A 1999 Dec 7;96(25):14523-8..
11. Yang D, Holt GE, Velders MP, Kwon ED, Kast WM. Murine six-transmembrane epithelial antigen of the prostate, prostate stem cell antigen, and prostate-specific membrane antigen: prostate-specific cell-surface antigens highly expressed in prostate cancer of transgenic adenocarcinoma mouse prostate mice. Cancer Res. 2001 Aug 1;61(15):5857-60..
12. Korkmaz KS, Elbi C, Korkmaz CG, Loda M, Hager GL, Saatcioglu F. Molecular cloning and characterization of STAMP1, a highly prostate-specific six transmembrane protein that is overexpressed in prostate cancer. J Biol Chem 2002;277(39):36689-96.
13. Challita-Eid PM, Morrison K, Etessami S, An Z, Morrison KJ, Perez-Villar JJ, et al Monoclonal antibodies to six-transmembrane epithelial antigen of the prostate-1 inhibit intercellular

communication in vitro and growth of human tumor xenografts in vivo. Cancer Res. 2007 Jun 15;67(12):5798-805.

14. Kobayashi H, Nagato T, Sato K, Aoki N, Kimura S, Murakami M, et al. Recognition of prostate and melanoma tumor cells by six-transmembrane epithelial antigen of prostate-specific helper T lymphocytes in a human leukocyte antigen class II-restricted manner. Cancer Res. 2007 Jun 1;67(11):5498-504.
15. Gomes IM, Maia CJ, Santos CR. STEAP proteins: from structure to applications in cancer therapy. Mol Cancer Res. 2012 May;10(5):573-87.
16. Gomes IM, Arinto P, Lopes C, Santos CR, Maia CJ. STEAP1 is overexpressed in prostate cancer and prostatic intraepithelial neoplasia lesions, and it is positively associated with Gleason score. Urol Oncol. 2014 Jan;32(1):53.e23-9.
17. Maia CJ, Socorro S, Schmitt F, Santos CR. STEAP1 is over-expressed in breast cancer and down-regulated by 17beta-estradiol in MCF-7 cells and in the rat mammary gland. Endocrine. 2008;34(1-3):108-16.
18. Cheung IY, Feng Y, Danis K, Shukla N, Meyers P, Ladanyi M, et al. Novel markers of subclinical disease for Ewing family tumors from gene expression profiling. Clin Cancer Res. 2007 Dec 1;13(23):6978-83.
19. Hayashi T, Oue N, Sakamoto N, Anami K, Oo HZ, Sentani K, et al. Identification of transmembrane protein in prostate cancer by the Escherichia coli ampicillin secretion trap: expression of CDON is involved in tumor cell growth and invasion. Pathobiology. 2011;78(5):277-84.
20. Moreaux J, Kassambara A, Hose D, Klein B. STEAP1 is overexpressed in cancers: a promising therapeutic target. Biochem Biophys Res Commun. 2012 Dec 14;429(3-4):148-55.
21. Lee CH, Chen SL, Sung WW, Lai HW, Hsieh MJ, Yen HH, et al. The Prognostic Role of STEAP1 Expression Determined via Immunohistochemistry Staining in Predicting Prognosis of Primary Colorectal Cancer: A Survival Analysis. Int J Mol Sci. 2016 Apr;17(4):592.
22. Yang Y, Xun N, Wu JG. Long non-coding RNA FGF14-AS2 represses proliferation, migration, invasion, and induces apoptosis in breast cancer by sponging miR-205-5p. Eur Rev Med Pharmacol Sci. 2019 Aug;23(16):6971-82.
23. Deep G, Singh RP, Agarwal C, Kroll DJ, Agarwal R. Silymarin and silibinin cause G1 and G2-M cell cycle arrest via distinct circuitries in human prostate cancer PC3 cells: a comparison of flavanone silibinin with flavanolignan mixture silymarin. Oncogene. 2006 Feb 16;25(7):1053-69.
24. Song Q, Qin S, Pascal LE, Zou C, Wang W, Tong H, et al. SIRPB1 promotes prostate cancer cell proliferation via Akt activation. The Prostate. 2020 Mar;80(4):352-64..
25. Chen Q, Gao Y, Yu Q, Tang F, Zhao PW, eta l. miR-30a-3p inhibits the proliferation of liver cancer cells by targeting DNMT3a through the PI3K/AKT signaling pathway. Oncol Lett. 2020;19(1):606-14.
26. Yu H, Yao J, Du M, Ye J, He X, Yin L. CDKN3 promotes cell proliferation, invasion and migration by activating the AKT signaling pathway in esophageal squamous cell carcinoma. Oncol Lett. 2020;19(1):542-8.

27. Hou B, Li W, Li J, Ma J, Xia P, Liu Z, et al. Tumor suppressor LHPP regulates the proliferation of colorectal cancer cells via the PI3K/AKT pathway. Oncol Rep. 2020 Feb;43(2):536-48.
28. Yun SH, Han SH, Park JI. COUP-TFII Knock-down Promotes Proliferation and Invasion in Colorectal Cancer Cells via Activation of Akt Pathway and Up-regulation of FOXC1. Anticancer Res. 2020;40(1):177-90.
29. Si X, Xu F, Xu F, Wei M, Ge Y, Chenge S. CADM1 inhibits ovarian cancer cell proliferation and migration by potentially regulating the PI3K/Akt/mTOR pathway. Biomed Pharmacother. 2019;123:109717.
30. Santamaria PG, Moreno-Bueno G, Portillo F, Cano A. EMT: Present and future in clinical oncology. Mol Oncol. 2017;11(7):718-38.
31. De Seta D, Mancini P, Minni A, Prosperini L, De Seta E, Attanasio G, et al. Bell's palsy: symptoms preceding and accompanying the facial paresis. ScientificWorldJournal. 2014;2014:801971.
32. Buccione R, Caldieri G, Ayala I. Invadopodia: specialized tumor cell structures for the focal degradation of the extracellular matrix. Cancer Metast Rev. 2009;28(1-2):137-49.
33. Egeblad M, Werb Z. New functions for the matrix metalloproteinases in cancer progression. Nat Rev Cancer. 2002;2(3):161-74.
34. Ghosh S, Basu M, Roy SS. ETS-1 protein regulates vascular endothelial growth factor-induced matrix metalloproteinase-9 and matrix metalloproteinase-13 expression in human ovarian carcinoma cell line SKOV-3. J Biol Chem. 2012;287(18):15001-15.
35. Liang Y, Xing X, Beamer MA, Swindell WR, Sarkar MK, et al. Six-transmembrane epithelial antigens of the prostate comprise a novel inflammatory nexus in patients with pustular skin disorders. J Allergy Clin Immunol. 2017;139(4):1217-27.
36. Yonemura Y, Ishibashi H, Hirano M, Mizumoto A, Takeshita K, Noguchi K, et al. Effects of Neoadjuvant Laparoscopic Hyperthermic Intraperitoneal Chemotherapy and Neoadjuvant Intraperitoneal/Systemic Chemotherapy on Peritoneal Metastases from Gastric Cancer. Ann Surg Oncol. 2017;24(2):478-85.

Tables

Table 1. The clinicopathological data of the 212 patients

Clinicopathological factors	Patients (%) 212 (100))	5-year OS (100%)	*P*-value
Sex			0.637
Male	161(75.9)	42.9	
Female	51 (24.1)	39.2	
Age (years)			0.675
≤60	103(48.6)	42.7	
>60	109 (51.4)	41.3	
Location			0.029
Upper	26 (12.3)	38.5	
Middle	29(13.7)	44.8	
Lower	143 (67.5)	44.8	
Entire	14 (6.6)	14.3	
Size (cm)			0.012
≤4	55 (25.9)	56.4	
>4	157 (74.1)	36.9	
Borrmann Type			0.019
Borrmann 1	8(3.8)	50.0	
Borrmann 2	14 (6.6)	78.6	
Borrmann 3	185(87.3)	39.5	
Borrmann 4	5 (2.3)	20.0	
Differentiation degree*			0.472
Differentiated	102 (48.1)	39.2	
Undifferentiated	110 (51.9)	44.5	
STEAP1 expression status			<0.001
Low	96 (45.3)	60.7	
High	116(54.7)	25.9	
Lymphovascular invasion			0.052
Negative	139(65.6)	61.5	

Positive	73(34.4)	32.9	
T staging			<0.001
T1-2	33 (15.6)	57.6	
T3	34(16.0)	58.8	
T4a	139(65.6)	35.3	
T4b	6 (2.8)	16.7	
N staging			<0.001
N0	51(24.1)	70.6	
N1	48 (22.6)	45.8	
N2	35(16.5)	45.7	
N3a	50(23.6)	24.0	
N3b	28(13.2)	10.7	
M0 or M1			0.005
M0	201(94.8)	43.3	
M1	11(5.2)	10.7	

* High and medium differentiated tubular adenocarcinoma and papillary adenocarcinoma were regarded as differentiated types; mucous adenocarcinoma, signet ring cell carcinoma, low and undifferentiated adenocarcinoma were regarded as undifferentiated types.

Table 2. Multifactorial analysis

Clinicopathological factors	Exp(B)	95%CI	*P*-value
Borrmann Type	0.934	0.783-1.114	0.449
Location	1.131	0.700-1.827	0.614
Size (cm)	0.919	0.573-1.473	0.725
STEAP1 expression status	2.203	1.468-3.300	<0.001
M0 or M1	1.329	0.652-2.707	0.433
T staging	1.512	1.132-2.020	0.005
N staging	1.343	1.162-1.553	<0.001
Lymphovascular invasion	1.214	0.838-1.759	0.304

Table 3

Clinicopathological factors	Positive (cases)	Negative (cases)	*P*-value
Sex			0.100
Male	78	83	
Female	18	33	
Age (years)			0.921
≤60	47	56	
>60	49	60	
Location			0.103
Upper	13	13	
Middle	14	15	
Lower	77	66	
Entire	12	2	
Size (cm)			0.510
≤4	27	28	
>4	69	88	
Borrmann Type			0.009
Borrmann 1	1	7	
Borrmann 2	4	10	
Borrmann 3	107	78	
Borrmann 4	4	1	
Differentiation degree*			0.823
Differentiated	47	55	
Undifferentiated	49	61	
Lymphovascular invasion			0.142
Negative	71	68	
Positive	45	28	
T staging			0.619
T1-2	18	15	
T3	16	18	

T4a	60	79	
T4b	2	4	
N staging			<0.001
N0	15	36	
N1	27	21	
N2	19	16	
N3a	32	18	
N3b	23	5	
M0 or M1			0.542
M0	92	109	
M1	4	7	

* High and medium differentiated tubular adenocarcinoma and papillary adenocarcinoma were regarded as differentiated types; mucous adenocarcinoma, signet ring cell carcinoma, low and undifferentiated adenocarcinoma were regarded as undifferentiated types.

Figures

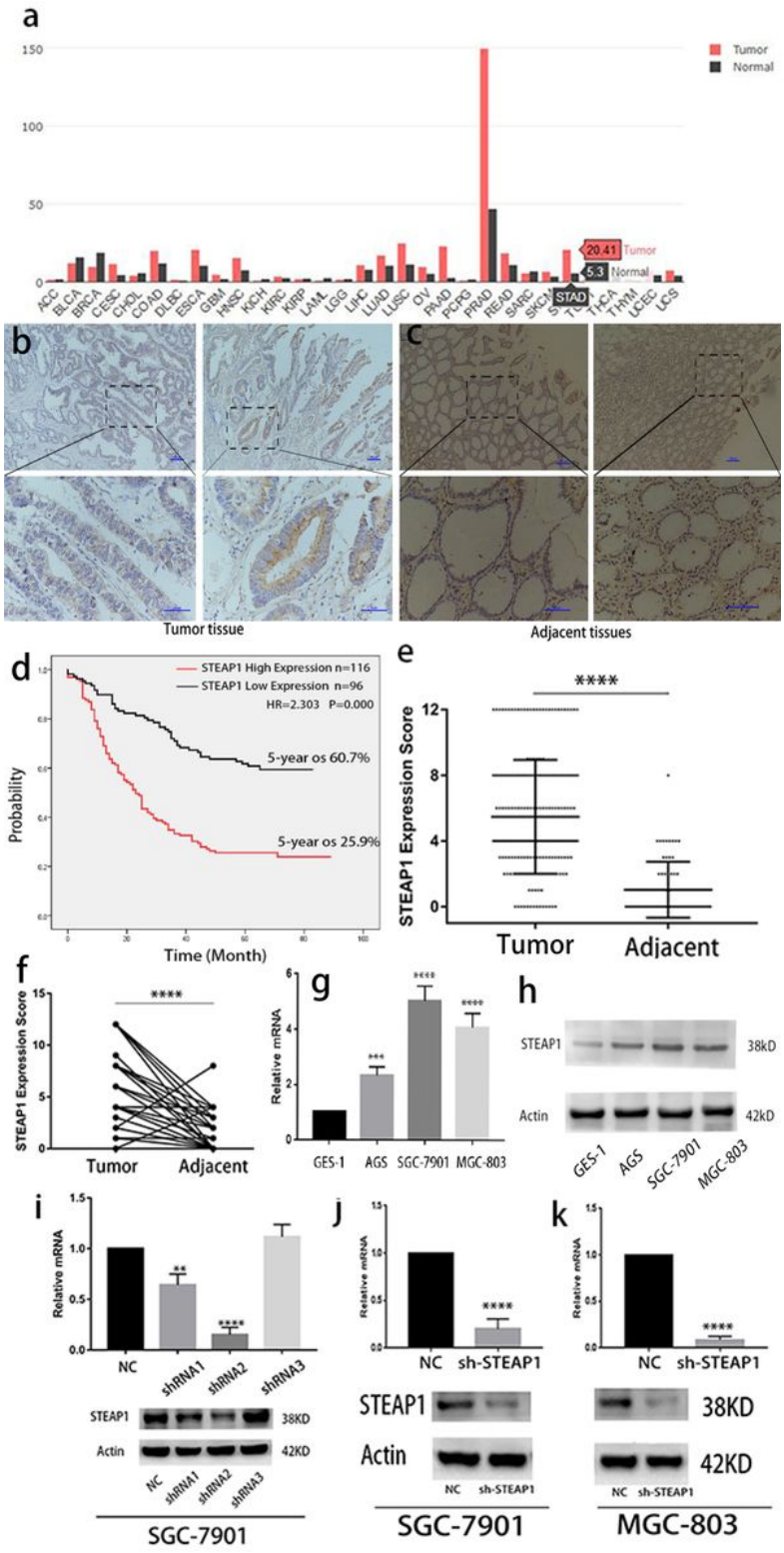

Figure 1

STEAP1 is highly expressed in gastric cancer and closely associated with OS; and STEAP1 lentivirus was successfully transfected into the cell line. (A) The GEPIA database shows the expression of STEAP1 in various types of cancer. (B) IHC assay shows the expression of STEAP1 protein in gastric cancer tissues (100x and 400x). (C) IHC assay shows the expression of STEAP1 protein in gastric paracancerous tissues (100x and 400x). (D) Kaplan-Meier analysis was used to show the overall survival rates in gastric cancer

patients with high and low expression levels of STEAP1. (E) The staining score distribution of 212 cases of gastric cancer and 60 cases of paracancerous tissues. (F) The staining score distribution of 60 matched tissues. (G) Detection of the expression of STEAP1 RNA expression levels in GES-1, AGS, SGC-7901 and MGC-803 cells. (H) Detection of the protein expression levels of STEAP1 in GES-1, AGS, SGC-7901 and MGC-803 cells. (I) Detection of the knockdown efficiency of three lentiviruses at the mRNA and protein levels using RT-PCR and Western blot analysis, respectively. (J) Detection of STEAP1 knockdown efficiency in the SGC-7901 cell line. (K) Detection of STEAP1 knockdown efficiency in the MGC-803 cell line. OS, overall survival. (*p<0.05, **p<0.01, ***p<0.001, ****p<0.0001)

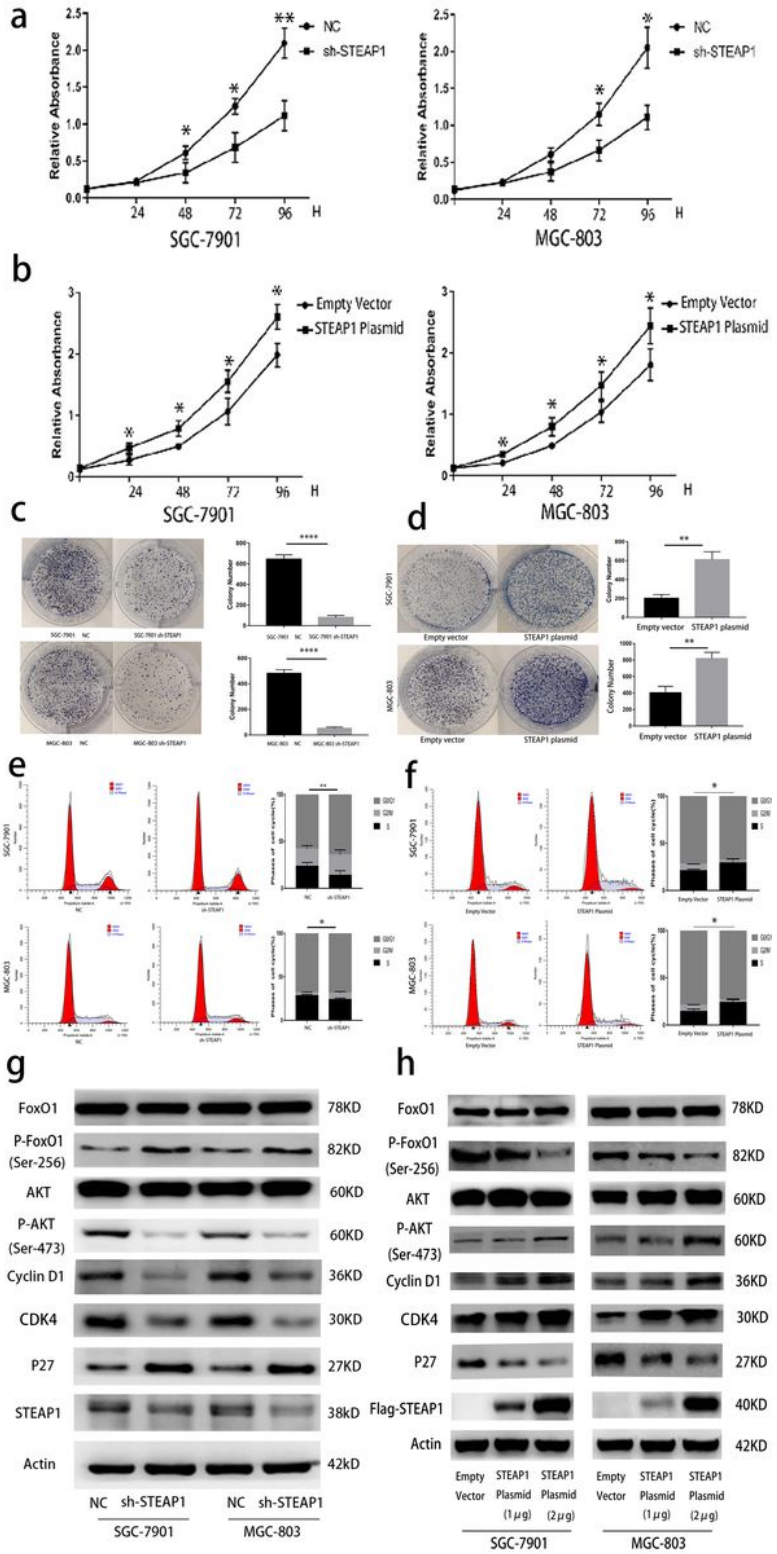

Figure 2

Functional experiments related to cell proliferation in the SGC-7901 and MGC-803 cell lines. (A) CCK-8 assay showed the differences in cell proliferation before and after knocking down STEAP1 in the SGC-7901 and MGC-803 cell lines. (B) CCK-8 assay showed the differences in cell proliferation before and after overexpression of STEAP1 in the SGC-7901 and MGC-803 cell lines. (C) Colony formation assay showed the differences in cell proliferation before and after knocking down STEAP1 in the SGC-7901 and

MGC-803 cell lines. (D) Colony formation assays showed the differences in cell proliferation before and after STEAP1 overexpression in the SGC-7901 and MGC-803 cell lines. (E) Flow cytometry detected the differences in cell cycle before and after knocking down STEAP1 in the SGC-7901 and MGC-803 cell lines. (F) Flow cytometry detected the difference in cell cycle before and after the overexpression of STEAP1 in the SGC-7901 and MGC-803 cell lines. (G) Western blot analysis detected the differences in protein expression related to the cell cycle and pathway before and after knocking down STEAP1 in the SGC-7901 and MGC-803 cell lines. (H) Western blot analysis detected the differences in protein expression related to the cell cycle and pathway before and after the overexpression of STEAP1 in the SGC-7901 and MGC-803 cell lines. (*p<0.05, **p<0.01, ***p<0.001, ****p<0.0001)

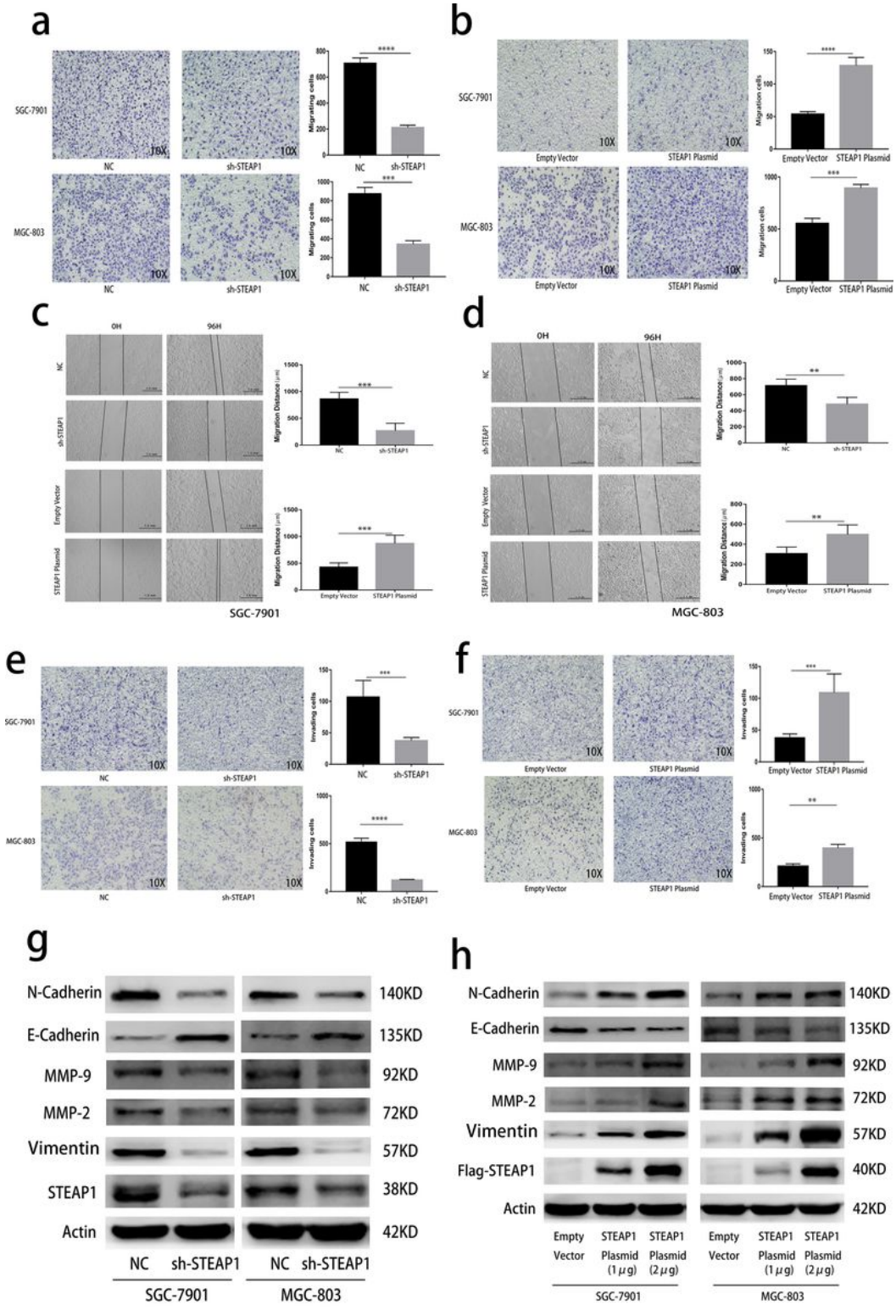

Figure 3

Functional experiments related to cell migration and invasion in the SGC-7901 and MGC-803 cell lines. (A) Detection of cell migration differences before and after knocking down STEAP1 in the SGC-7901 and MGC-803 cell lines using transwell assay. (B) Detection of cell migration differences before and after the overexpression of STEAP1 in the SGC-7901 and MGC-803 cell lines by transwell assay. (C) Detection of cell migration differences before and after knocking down STEAP1 in the SGC-7901 and MGC-803 cell

lines using wound healing assay. (D) Detection of cell migration differences before and after the overexpression of STEAP1 in the SGC-7901 and MGC-803 cell lines using wound healing assay. (E) Detection of cell invasion differences before and after knocking down STEAP1 in the SGC-7901 and MGC-803 cell lines using transwell assay. (F) Detection of cell invasion differences before and after the overexpression of STEAP1 in the SGC-7901 and MGC-803 cell lines using transwell assay. (G) Western blot analysis detected the difference in protein expression related to cell migration, invasion and EMT before and after knocking down STEAP1 in the SGC-7901 and MGC-803 cell lines. (H) Western blot analysis detected the difference in protein expression related to cell migration, invasion and EMT before and after the overexpression of STEAP1 in the SGC-7901 and MGC-803 cell lines. (*p<0.05, **p<0.01, ***p<0.001, ****p<0.0001)

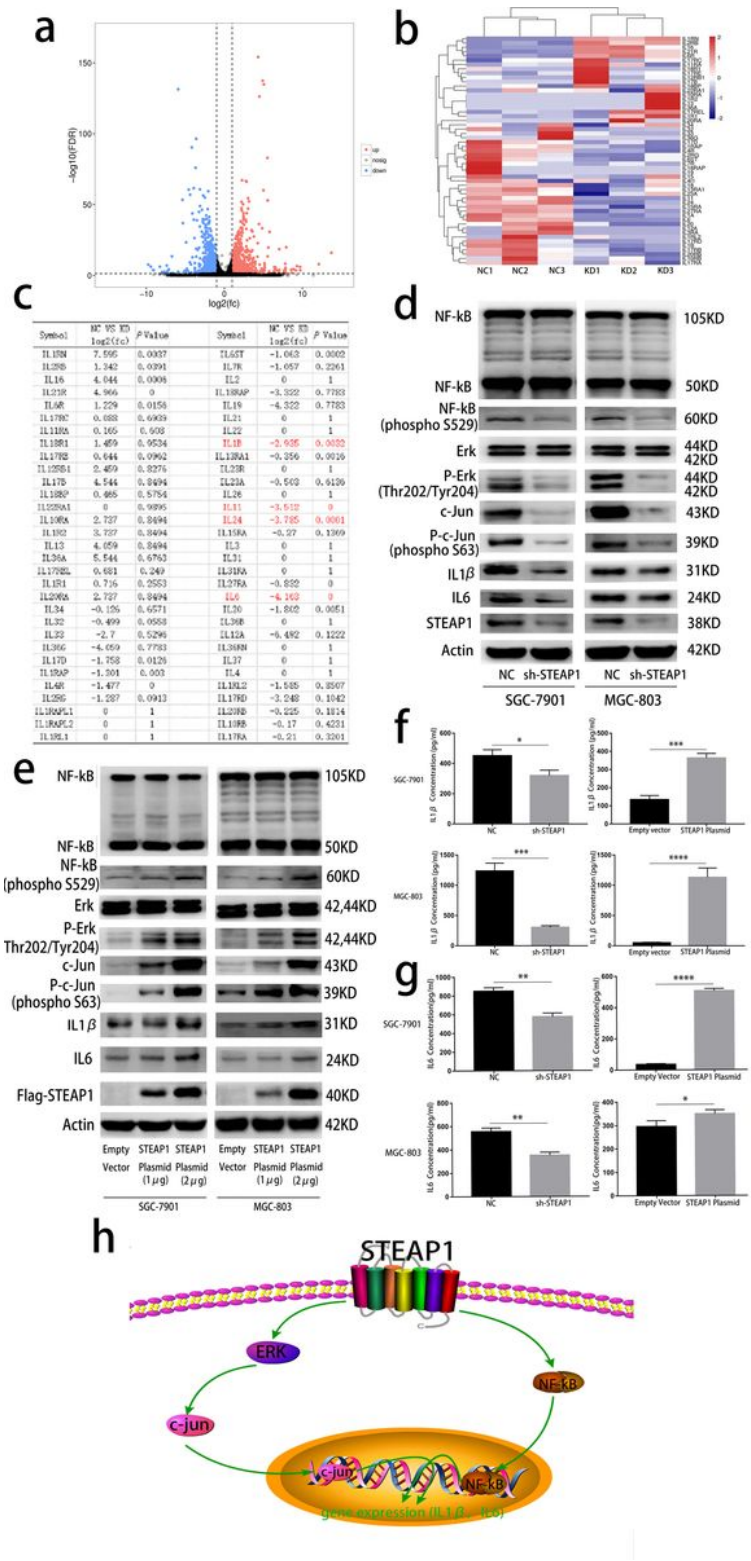

Figure 4

The results of RNA-seq and detection of inflammation-related pathway proteins. (A) The volcano map shows some differentially expressed genes between the SGC-7901 NC and sh-STEAP1 groups. (B) The RNA-seq results showed the inflammation-related gene expression differences between the SGC-7901 NC and the sh-STEAP1 groups through heat map analysis. (C) Numerical display of differences in inflammatory related factors. (D) Western blot analysis detected the protein expression differences of

IL1β, IL6 and upstream related pathway proteins before and after knocking down STEAP1 in the SGC-7901 and MGC-803 cell lines. (E) Western blot analysis detected the protein expression differences of IL1β, IL6 and upstream related pathway proteins before and after the overexpression of STEAP1 in the SGC-7901 and MGC-803 cell lines. (F) Detection of differences in IL1β protein secretion capacity between different processing states in the SGC-7901 and MGC-803 cell lines using ELISA. (G) Detection of differences in IL6 protein secretion capacity between different processing states in the SGC-7901 and MGC-803 cell lines using ELISA. (h) STEAP1 mediated the inflammatory response by regulating IL1β and IL6 via the NF-kB and ERK/c-Jun pathways. (*p<0.05, **p<0.01, ***p<0.001, ****p<0.0001)

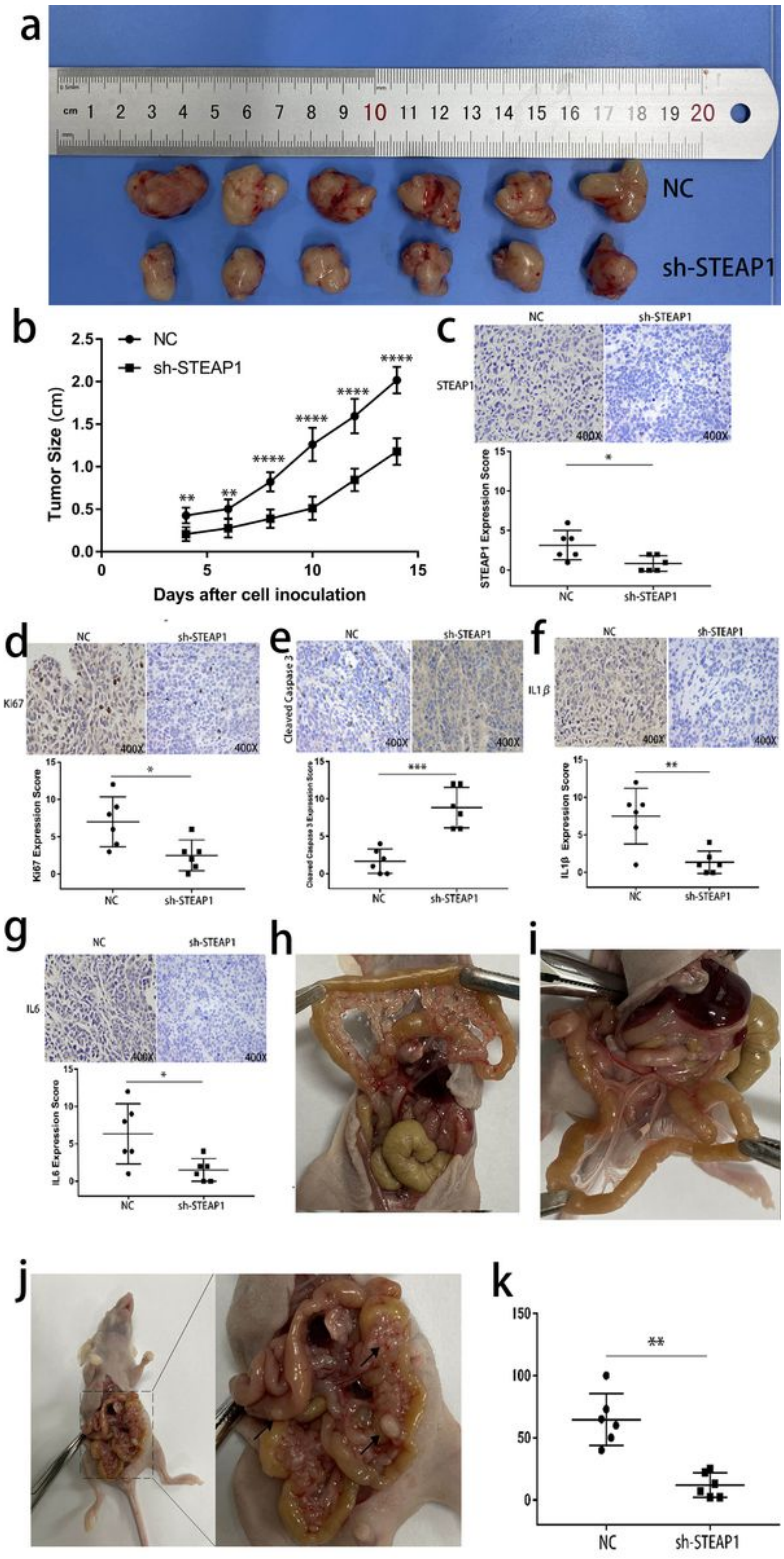

Figure 5

The effect of the STEAP1 gene on cell proliferation and peritoneum implantation in vivo through animal experiments. (A) The tumorigenesis experiment in nude mice shows the differences in tumor size between the SGC-7901 NC and sh-STEAP1 groups. (B) The difference in tumor size between the SGC-7901 NC and sh-STEAP1 groups in two weeks. (C) IHC assay shows the expression of STEAP1 in the tumors in nude mice (400x). (D) IHC assay shows the expression of Ki-67 in the tumors in nude mice

(400x). (E) IHC assay shows the expression of cleaved caspase3 in the tumors in nude mice (400x). (F) IHC assay shows the expression of IL1β in the tumors in nude mice (400x). (G) IHC assay shows the expression of IL6 in the tumors in nude mice (400x). (H) The distribution and quantity of tumor in abdominal cavity in the NC group. (G) Distribution and quantity of tumor in abdominal cavity in the sh-STEAP1 group. (J) The tumors were mainly located on the mesentery and the intestinal wall. (K) The comparison of tumor number between SGC-7901 NC and sh-STEAP1 groups. IHC, immunohistochemistry